LUND UNIVERSITY

Identification of fibroblast growth factor-8b target genes associated with early and late cell cycle events in breast cancer cells.

Nilsson, E M; Brokken, Leon; Narvi, E; Kallio, M J; Härkönen, Pirkko

Link to publication

Total number of authors:
5

Identification of fibroblast growth factor-8b target genes associated with early and late cell cycle events in breast cancer cells

Nilsson EM[a], Brokken LJS[a], Narvi E[c,d], Kallio[c,d], MJ and Härkönen PL[a,b]

[a]Department of Laboratory Medicine, Tumor Biology, Lund University, Sweden
[b]Institute of Biomedicine, Department of Cell Biology and Anatomy, University of Turku, Finland
[c]Turku Centre for Biotechnology, University of Turku, Finland
[d]VTT Technical Research Centre of Finland, Biotechnology for Health and Wellbeing, Turku, Finland

Email addresses: Emeli.Nilsson@med.lu.se, Leon.Brokken@med.lu.se, Elli.Narvi@vtt.fi, marko.kallio@vtt.fi and Harkonen@utu.fi

Running head: FGF-8b-regulated genes in breast cancer

Address correspondence to: Emeli Nilsson, Department of Laboratory Medicine, Tumor Biology, Lund University, CRC, Building 91, Plan 10, Entrance 72, SUS, 205 02 Malmö, Sweden. Telephone number: +46704800926; Fax number: +46 40 391222; E-mail: Emeli.Nilsson@med.lu.se

ABSTRACT

Fibroblast growth factor-8 (FGF-8) is implicated in the development and progression of breast cancer and its levels is frequently elevated in breast tumors. The mechanisms driving FGF-8-mediated tumorigenesis are not well understood. Herein we aimed to identify target genes associated with FGF-8b-mediated breast cancer cell proliferation by carrying out a cDNA microarray analysis of genes expressed in estrogen receptor negative S115 breast cancer cells treated with FGF-8b for various time periods in comparison with those expressed in non-treated cells. Gene and protein expression was validated for selected genes by qPCR and western blotting respectively. Furthermore, using TRANSBIG data, the expression of human orthologs of FGF-8-regulated genes was correlated to the Nottingham prognostic index and estrogen receptor status. The analysis revealed a number of significantly up- and down regulated genes in response to FGF-8b at all treatment times. The most differentially expressed genes were genes related to cell cycle regulation, mitosis, cancer, and cell death. Several key regulators of early cell cycle progression such as Btg2 and cyclin D1, as well as regulators of mitosis, including cyclin B, Plk1, survivin, and aurora kinase A, were identified as novel targets for FGF-8b, some of which were additionally shown to correlate with prognosis and ER status in human breast cancer. The results suggest that in stimulation of proliferation FGF-8b not only promotes cell cycle progression through the G1 restriction point but also regulates key proteins involved in chromosomal segregation during mitosis and cytokinesis of breast cancer cells.

2

1. Introduction

The fibroblast growth factor (FGF) family comprises 22 members of multifunctional

polypeptide growth factors that are involved in a variety of processes including embryonic

differentiation, mitogenesis, angiogenesis, and wound healing. Recent studies have linked the

expression of certain FGFs and FGF receptors to tumorigenesis (Dorkin et al., 1999; Giri et

al., 1999; Katoh and Katoh, 2009; Marzioni et al., 2009).

Fibroblast growth factor-8 (FGF-8) is expressed at a high level in a large proportion of

breast cancers (Marsh et al., 1999). Experimental data suggests that FGF-8 is associated with

development and progression of breast cancer (Mattila and Harkonen, 2007). Mice over

expressing FGF-8 have provided evidence that FGF-8 contributes to mammary gland

tumorigenesis (Daphna-Iken et al., 1998) and over expression of FGF-8 in murine S115 cells

and human MCF-7 cells leads to increased tumor growth and angiogenesis in nude mice

(Mattila et al., 2001; Ruohola et al., 2001). Our data and the data of others clearly indicate a

role for FGF-8 in breast tumorigenesis. However, the mechanisms by which FGF-8 induces

transformation are not well characterized.

Alternative splicing of the FGF-8 gene can give rise to eight potential protein

isoforms in mouse, FGF-8 a-h, and four isoforms in humans, FGF-8 a, b, e, f (Gemel

et al., 1996). Although isoforms a and e have weak transforming capacity, isoform b

is the isoform that has the strongest transforming capacity and also the highest affinity

for the FGF receptors (Olsen et al., 2006) and is therefore the isoform of most

importance in breast tumorigenesis.

We have previously characterized the pathways associated with FGF-8b-induced

proliferation of breast cancer cells. Like many growth factors, FGF-8b stimulates cell cycle

progression and proliferation by enhancing cyclin D1 transcription via the ERK/MAPK and

PI3K/Akt pathways. Apart from stimulating proliferation, FGF-8b contributes to expansion of

breast cancer cell populations by acting as a survival factor (Nilsson et al., 2010). In this study

we aim to clarify the mechanistic action of FGF-8b in the development and progression of

breast cancer and accordingly we investigated the transcriptional changes associated with FGF-8b stimulation of estrogen receptor negative S115 mouse breast cancer cells using cDNA microarray analysis.

A large number of differentially expressed genes associated with FGF-8b were identified and analysis of the most differentially expressed genes revealed their involvement in cellular processes such as cell cycle regulation, mitosis, cancer, and cell death. Moreover, the expression of human orthologs of several FGF-8b-regulated genes, such as cyclin B, cyclin A, aurora kinase A, aurora kinase B, Polo-like kinase 1 (Plk1) and Dual specificity phosphates 4 (DUSP4) correlated in a statistically significant way with Nottingham prognostic index (NPI) and estrogen receptor (ER) status in human breast cancers.

2. Material and methods

2.1 Cell culture

Shionogi 115 (S115) mouse mammary tumor cells were maintained in DMEM culture medium (GIBCO, Paisley, UK) supplemented (4%) with heat-inactivated fetal bovine serum (FBS) and 10 nM testosterone (Sigma-Aldrich, St. Louis, MO). For experiments with FGF-8b, cells were pre-cultured for 48 h in DMEM supplemented with 4% dextran-charcoal stripped FBS (dcFBS) in order to deprive cells of testosterone and growth factors. The cells were washed twice with PBS and the medium was replaced with Ham's F-12 (GIBCO) containing bovine serum albumin (BSA; 0.2%) and mouse recombinant FGF-8b protein (25 ng/ml; R&D Systems, Abingdon, UK) or PBS vehicle (control). After various time periods of FGF-8b stimulation, cells were harvested for either RNA or protein extraction. Cells were cultured in a humidified incubator at 37 °C in 5% CO_2.

2.2 Oligonucleotide microarrays

Oligonucleotide microarrays were produced at the Swegene DNA Microarray Resource Center, Department of Oncology, Lund University, Sweden. The mouse array-ready oligonucleotide library Version 4.0, containing approximately 35 000 probes, were obtained

from Operon (Operon Biotechnologies, Germany). Probes were dissolved in Corning

Universal spotting solution (Corning, Acton, MA) and printed on glass slides.

2.3 RNA preparation and cDNA synthesis

For cDNA microarray analysis, S115 cells were treated with FGF-8b or PBS vehicle for

1, 3, 6, 12 and 24 h. Total RNA was extracted using Trizol (Invitrogen, Carlsbad, CA)

followed by RNA purification on Qiagen RNeasy columns (Qiagen). Sample integrities were

assessed on an Agilent 2100 Bioanalyzer (Agilent technologies, Palo Alto, CA). Five µg of

total RNA was reverse-transcribed to cDNA using a biotinylated oligo-dT primer with

universal PCR sequence. For each time point cDNA samples were prepared in triplicate.

2.4 Labeling and cDNA microarray hybridizations

cDNA was fluorescently labeled with Cy3-dCTP and Cy5-dCTP (Amersham

Biosciences, Uppsala, Sweden) using the Pronto! Plus Direct Labeling v1.9 kit (Corning Life

Sciences, Corning, NY) according to manufacturer's instructions. FGF-8b-treated samples

and control samples were labeled with both Cy3 and Cy5 to make dye swap hybridizations.

Differentially labeled cDNA from FGF-8b samples and control samples were combined and

dissolved in Pronto! Universal Hybridization Solution (Corning Life Sciences). Hybridization

reactions were applied to microarrays and incubated at 42 °C for 18 hours using a water bath.

Fluorescence of the hybridized microarrays was recorded using an Agilent G2565AA

microarray scanner (Agilent Technologies).

2.5 Microarray and data analysis

Primary hybridization data was collected using GenePix Pro 4.0 software (Axon

Instruments, Foster City, CA) and raw data files were uploaded into BioArray Software

Environment (BASE) version 1.2.17 (Saal et al., 2002). In BASE, spots were background-

corrected using the median foreground minus the median background signal intensity for both

dyes and the fluorescence ratios between FGF-8 treated samples and control samples were

calculated. Unreliable features and spots not showing signal-to-noise ratios ≥3, for both channels, were removed. Data was normalized within each array using Lowess curve fitting. Analysis was restricted to genes present on >80 percent of the arrays after filtering. Gene lists of up- or down regulated genes were created in BASE at FDR<0.01.

Significance analysis of microarrays (SAM) as implemented in MeV v4.1 (Saeed et al., 2003) was used to identify genes with significantly altered expression (FDR<0.01) during the 1-24 h time course. The 400 most significantly altered genes were applied to Ingenuity Pathways Analysis software (IPA; Ingenuity systems Inc., Redwood City, CA) to identify categories and canonical pathways associated with FGF-8b. A cut-off value of less than or equal to a probability score of 0.2 was set as the threshold for selection of genes of interest. For canonical pathways, P values were calculated by IPA using Fischer's exact test, which is a measure of the probability that the selected genes are associated with a pathway by chance alone.

2.6 Validation of gene expression by quantitative PCR

S115 cells were stimulated with FGF-8b as described above and after indicated time periods, total RNA was isolated using Trizol (Invitrogen). Two μg of total RNA was reverse-transcribed using First-Strand cDNA Synthesis Kit according to the manufacturer's instructions (GE Healthcare, UK). The resulting cDNA was used as a template for quantitative PCR amplification using DyNAmo SYBR green qPCR Kit (Finnzymes Oy, Finland) under the following conditions: initial denaturation at 95 ºC for 10 min followed by 40 cycles of denaturation at 95 ºC for 30 s, annealing at 56 ºC for 1 min and extension at 72 ºC for 1 min. The mouse and human primers sequences used in qPCR are presented in Supplemental Table 1. Relative mRNA expression levels were calculated as a ratio to β-actin mRNA levels.

2.7 siRNA treatment

 S115 cells were seeded in pre-culture medium such that they were 30-50% confluent at the time of transfection 24 h later. Medium was replaced with Ham's F-12 containing BSA (0.2%) prior to transfection. On-Targetplus Smartpool siRNAs targeting Btg2, cyclin D1 and aurora kinase A and (Dharmacon RNA Technologies, Lafayette, CO) were diluted in OptiMEM (GIBCO) and complexed with Lipofectamine 2000 (Invitrogen) to a final concentration of 40 nM oligonucleotides. The oligomer-Lipofectamine 2000 complex was subsequently added to the medium. Five hours after transfection, medium was replaced with Ham's F-12 containing BSA (0.2%) and FGF-8b (25 ng/ml). Cells were harvested for protein expression analysis by western blotting and for cell viability measurements by the trypan blue exclusion assay. Cells transfected with Non-Target plus sicontrol pool were used as a negative control. The statistical differences between treatments were tested using one-way ANOVA followed by Bonferroni's multiple comparison tests. $P<0.05$ was considered statistically significant.

2.8 Western blotting

 Cells were washed twice with ice-cold PBS and lysed in ice-cold lysis buffer (Biosource, Camarillo, CA). Proteins were separated by SDS-PAGE, transferred to polyvinylidene difluoride membranes (Millipore Corporation, Bedford, USA) and probed with primary antibodies against BTG2, cyclin D1, cyclin B1 (1:1000; Cell Signaling Technology, Beverly, MA), Plk1 (0.4 μg/ml; Santa Cruz Biotechnology, Inc., Santa Cruz, CA), aurora kinase A (4.6 μg/ml; Abcam, Cambridge, UK) and β-actin (0.5 μg/ml; Sigma, St. Louis, MO). Secondary antibodies used were goat anti-rabbit and goat anti-mouse (Pierce Biotechnology, Inc., Rockford, USA) conjugated with horseradish peroxidase. Antibody binding was visualized using Super Signal West Dura Chemiluminescent Substrate (Pierce Biotechnology).

2.9 Immunohistochemistry

Formalin-fixed paraffin-embedded tissue sections of S115-FGF-8b tumors (Mattila et al., 2001) and MCF-7-FGF-8b tumors (Ruohola et al., 2001) were deparaffinized with xylene and rehydrated through a graded series of ethanol and a final wash in distilled water. To inhibit endogenous peroxidase activity, the sections were incubated with 3% hydrogen peroxide in methanol for 10 minutes. They were then rinsed three times in distilled water. Antigen retrieval was achieved with immersion in Tris/EDTA (10mM Tris Base, 1mM EDTA, pH 9.0) and heated in a microwave oven for 15 minutes. The slides were left to cool for 20 minutes before being washed with PBS and 0.1% Tween-20 (PBST). Sections were blocked with 1% BSA in PBST containing 10% normal serum for 30 minutes and then incubated with aurora kinase A (2.3 μg/ml; Abcam) antibodies in 1% BSA-PBST at 4ºC overnight. The slides were rinsed three times in PBST followed by 30 minutes' incubation with biotinylated anti-rabbit IgG or anti-goat IgG (3.8 μg/ml; Vector Laboratories, USA). They were rinsed three times in PBST and labeled by using a Vectastain ABC Kit (Vector Laboratories) according to the manufacturer's instructions. After three rinses in PBS, antibody binding was visualized by incubating the sections in 3,3'-diaminobenzidine (DAB Kit, Vector Laboratories) for 3-5 minutes. The slides were rinsed in distilled water and thereafter in tap water. All sections were counterstained with haematoxylin and coverslipped with Mountex mounting medium (Histolab, Sweden). The sections were viewed and analyzed using a x40 objective on an Olympus IX70 microscope equipped with an Olympus DP70 digital camera.

2.10 Analyses of mitotic and micronuclei indices and duration of cell division

S115 cells were cultured in 96-well plates as indicated above. The cells were either stimulated with FGF-8b or grown without the growth factor. The cells in the 96-well plates were monitored using incucyte imaging system (Essen Instruments, Welwyn Garden City, UK) for a total of 96 hours by taking still images at 10-60 min intervals pending of the experiment. Time-lapse films were built of the still images and the duration of mitosis was

determined as averages from pools of 30 mitotic cells per each assay condition in three replicates. In this study, duration of mitosis was defined as the time from nuclear envelope breakdown to end of telophase. The mitotic indices were determined from the same cell populations cultured in various growth conditions by calculating the frequency of M phase cells within a population of 1000 cells per assays condition in three replicates. In a separate set of assays the frequency of micronuclei was determined using fixed and DNA stained cell populations grown in various culture conditions. In short, the cells grown in 96-well plates were fixed with 4% paraformaldehyde for 7 min at RT prior to permeabilisation (1%BSA + 0,5 % Triton x-100) for 30 min at RT. The DNA was stained using DAPI and the frequency of micronuclei was calculated using Olympus ScanR microscope with a 20 x objective equipped with Hamamatsu ORCA-ER CCD camera. The micronucleus results are average from three replicate samples each having a total of 1000 cells analysed.

2.11 Statistical analysis of TRANSBIG data

Microarray data for TRANSBIG breast cancer tumors (Desmedt et al., 2007) was retrieved from GEO-database (GSE7390). The series represents samples from 198 lymph node-negative breast cancer patients. In short, samples were hybridized onto Affymetrix Human Genome U133A Array, and data was processed and normalized using MAS 5.0 algorithms as reported in the GEO database. Data analysis and visualization of GSE7390 data was performed using the statistical programming language R (version 2.9.1) (Team, 2009), and its specific package collection for bioinformatics Bioconductor (version 2.4.1) (Gentleman et al., 2004). Every analysis was made using the log2-transformed data. Selected mouse genes were mapped to U133A human gene probe sets using HomoloGene database. A total of 592 probe sets from U133A array were identified as orthologs and used in future analysis. Data from 592 probe sets and 198 tumor samples were clustered with hierarchical clustering using Euclidian metrics and complete linkage clustering algorithm. Gene sets showing differential expression between two main patient clusters were selected for further analysis.

Expression of selected genes and the Nottingham prognostic index (NPI) values as well as the estrogen receptor (ER) status of the tumors were visualized using box plots, each box presenting the distribution of expression values for a given NPI range. NPI is a clinicopathological classification system based on tumor size, histological grade and lymph node status used for breast cancer prognostication (Balslev et al., 1994; Elston and Ellis, 1991; Galea et al., 1992; Sauerbrei et al., 1997; Todd et al., 1987). Patients with NPI ≤ 3.4 are considered to have a good prognosis, patients with 3.4 < NPI ≤ 5.4 a moderate prognosis and patients with NPI > 5.4 are considered to have a poor prognosis (Todd et al., 1987).

ER status is another important prognostic factor for breast cancer patients. Patients with ER expressing (ER positive) tumors generally have a more favorable outcome than patients with non- or low-expressing (ER negative) tumors. The difference of mean gene expression between the categorized NPI values and between ER negativity and positivity was tested using analysis of variance (ANOVA) and Student´s t test, respectively. Additionally, the correlation between the expression of individual genes and NPI values was calculated using Pearson's product-moment correlation coefficient and the statistical significance was tested using Fisher's Z transform.

3. Results

3.1 Genes up regulated and down regulated by FGF-8b

Using the normalized data from the cDNA microarrays, gene lists were generated in BASE 2.14.1 for up- and down regulated genes in breast cancer cells treated with FGF-8b for 1, 3, 6, 12, and 24 h, in comparison with untreated cells. Significance was assigned using a False Discovery Rate (FDR) threshold of 1%. Cells treated with FGF-8b for 1 hour generated a data set of 4 significantly up regulated genes and 5 down regulated genes (Supplemental Table 2). Three hours of FGF-8b treatment generated 76 up regulated genes and 21 down regulated genes and 6 hours of FGF-8b treatment generated 40 up regulated genes and 34 down regulated genes. Twelve hours of FGF-8b treatment resulted in a larger set of differentially expressed genes: 76 up regulated genes and 80 down regulated genes, and 24 h

generated the largest number of differentially expressed genes: 209 up regulated genes and 169 down regulated genes.

3.2 FGF-8b target genes regulate cell cycle, cancer and cell death.

After identifying the most up and down regulated genes following FGF-8b treatment at single time points, we performed a significance analysis of microarrays (SAM) to identify genes with significantly altered expression during the 1-24 hour time course, taking all time points into account. The 20 most significantly altered genes are presented in Table 1. To understand the function of the FGF-8b-regulated genes and their roles in biological processes we used the 400 most significantly altered genes (Supplemental Table 3) derived from SAM and applied them to Ingenuity Pathway Analysis (IPA). The IPA identified 60 categories associated with FGF-8b-regulated genes with P values less than 0.01 (Supplemental Table 4). The five highest ranked categories, which are shown in Table 2, indicate that the FGF-8b-regulated genes are primarily involved in cell cycle, cancer, cellular growth and proliferation, cell death, and tumor morphology.

The IPA also identified eleven canonical pathways associated with FGF-8b-regulated genes with P values less than 0.01. Table 3 shows the eleven pathways and their associated genes. Two of the canonical pathways, mitotic roles of polo-like kinase and cell cycle regulation by Btg family proteins, are shown in Supplemental Figure 1 with up regulated genes depicted in red and the down regulated genes depicted in green. Symbols of differentially expressed genes (depicted in red or green) at different time points have been superimposed in order to illustrate the changes in their expression over time.

3.3 Validation of gene expression microarray data in S115 and MCF-7 cells by quantitative PCR.

As a result of the above analysis we found a number of particularly interesting genes which we chose for further investigation in regard to FGF-8b regulation. Figure 1a shows the

11

relative gene expression of Btg2, cyclin D1, cyclin B1, Plk1, aurora kinase A and Dusp4, as measured by the cDNA microarrays. The data of the microarrays were validated by measuring mRNA levels in FGF-8b treated S115 cells (Figure 1b) using qPCR. We further validated the microarray data by performing qPCR analysis on FGF-8b-treated MCF-7 human breast cancer cells (Figure 1c). Although the time and the magnitude of expression differ between the analyses, the expression pattern of the target genes identified in the microarray is largely replicated in the qPCR data derived from both S115 and MCF-7 cells. Btg2 expression is down regulated 3-6 hours after FGF-8b while cyclin D1 and Dusp4 gene expression is highly up regulated at 3 hours and onwards, peaking at 6-12 hours after FGF-8b addition. Cyclin B1, Plk1 and aurora kinase A gene expression levels rise moderately in response to FGF-8b and only at 12-24 hours after growth factor addition.

3.4 Validation of gene expression microarray data at protein level.

FGF-8b regulation was further analyzed at the protein level for BTG2, cyclin D1 cyclin B1, Plk1, aurora kinase A and Dusp4 in S115 cells. In agreement with increased mRNA levels caused by FGF-8b treatment, cyclin D1, cyclin B1, Plk1 and aurora kinase A protein levels were considerably increased by FGF-8b at both 12 and 24 hours (Fig. 2a). Knocking down cyclin D1, which we previously identified as an FGF-8b target gene (Nilsson et al., 2010), decreased but did not abolish the effect of FGF-8b on cyclin B1 and aurora kinase A protein levels at the 12 hour time point. At 24 h, cyclin D1-silencing did not influence the effect of FGF-8b on cyclin B1 and aurora kinase A protein levels. Plk1 induction by FGF-8b was however blocked in cyclin D1-silenced cells. No obvious regulation by either FGF-8b or cyclin D1 was detected in BTG2 protein expression at the measured time points. Dusp4 protein was expressed at high levels in S115 cells, but no regulation by FGF-8b was detected (data not shown).

Aurora kinase A, which is critically involved in regulation of mitosis, particularly in the formation of the mitotic spindle, was also studied by immunohistochemistry in nude mouse tumors formed by FGF-8b- and mock-transfected S115 and MCF-7 cells previously produced

in our group (Mattila et al., 2001; Ruohola et al., 2001). Aurora kinase A immunoreactivity

was primarily located in the nucleus, however, cytoplasmic localization of aurora kinase A

was also observed in both S115 and MCF-7 tumors (Fig 2b). The number of cells staining

positively for aurora kinase A in S115-FGF-8b tumors (upper right panel) was higher than in

S115-mock tumors (upper left panel). Similarly, FGF-8b increased aurora kinase A

immunostaining in MCF-7 tumors (lower right panel), although the difference between them

and control tumors (lower left panel) was not as obvious as for S115 tumors.

3.5 Examination of the mitotic progression and fidelity upon FGF-8b stimulation

To determine whether FGF-8b stimulation causes M phase delay in short term culture

we calculated the mitotic indices and analyzed the duration of cell division in FGF-8b

stimulated and control populations of mouse S115 cells. The treatment of S115 cells with

FGF-8b caused a significant threefold (P=0.008) increase in the mitotic index when compared

to the non-stimulated cells (Figure 3a). The average mitotic index was $6.6 \pm 0.6\%$ in the FGF-

8b treated cell populations versus $2.3 \pm 0.1\%$ in the non-stimulated control populations. To

exclude the possibility that the observed elevation of mitotic index in the FGF-8b treated cells

is not due to an M phase delay we measured the average duration of cell division in S115 cells

grown in the presence or absence of FGF-8b. The average length of mitosis was very similar

in both cell populations (Figure 3b); 76 ± 12 min in the FGF-8b treated cell populations and

69 ± 14 min in the non-stimulated control cell populations (P=0.063). These results strengthen

the notion that FGF-8b treatment triggers the cell cycle progression in the S115 cells indicated

by the increased mitotic index but on the other hand does not cause accumulation of cells into

M phase or delays in average duration of cell division.

Next we wanted to examine if the FGF-8b treatment has an effect on the mitotic fidelity.

To this end, we determined the frequency of micronuclei in the FGF-8b and control cell

populations. Micronuclei are small round DNA-stain positive cytoplasmic bodies near the

main nucleus of a divided cell. Micronuclei can contain either acentric chromosome

fragment(s) or whole chromosome(s) depending on the mitotic error the mother cell

13

experienced. No statistical difference was observed in the micronuclei frequency between the FGF-8b and control cell populations (P=0.155) proposing the cells undergo an error-free mitosis in both growth conditions (Figure 3c).

3.6 Silencing of FGF-8b target genes reduces FGF-8b-induced cell proliferation.

Next we wanted to determine whether silencing FGF-8b target genes affects FGF-8b-regulated cell proliferation and cell death. In previous work we showed that silencing cyclin D1 expression with siRNA reduces FGF-8b-induced proliferation in S115 cells (Nilsson et al., 2010). Similarly, silencing Btg2 and Aurora kinase A with siRNA (Figure 4a and b, left panel) reduced FGF-8b-induced cell proliferation significantly in S115 cells (Figure 4a, right panel).

Previously we also showed that FGF-8b promotes survival of S115 cells (Nilsson et al., 2010). To determine whether cyclin D1 is also critical for FGF-8b promotion of S115 cell survival we studied the ability of FGF-8b to rescue cyclin D1-siRNA-treated cells (Figure 4c, left panel) from undergoing cell death. Cells were pretreated with staurosporine (STS) in order to induce cell death. The survival effect of FGF-8b did not differ significantly in cyclin D1-silenced cells from that in control cells (Figure 4c, right panel) suggesting that cyclin D1 is not involved in the mechanisms mediating FGF-8b effects on cell survival.

3.7 Correlation between NPI and ER status in human breast cancers and expression of FGF-8b-regulated genes.

Using the 400 most significantly altered genes from our microarray analysis, as determined by SAM, 592 human orthologous probes were identified. Gene expression data of the 592 probes and Nottingham prognostic index (NPI) of 198 human breast cancer samples (Desmedt et al., 2007) were clustered. According to NPI two main patient clusters (high and low) were formed. A high NPI is associated with poor prognosis (Todd et al., 1987). Three gene sets that showed clearly different gene expression patterns in the two main patient clusters were selected for further study (Supplemental Figure 2). Mean expression of the

14

genes in the three gene sets (A-C) according to different NPI categories are shown in Figure 4a-c (left panels) as box plots. The genes belonging to each gene set are indicated below the box plot. The genes of each gene set are also shown in Supplemental Table 5 with their corresponding P-value and correlation coefficient. The difference between the mean gene expression values of the groups of categorized NPI values was statistically significant ($P<0.001$). Also, the correlation between the expression and NPI value was statistically significant for individual genes in each of the three clusters ($P<0.001$). Gene expression levels of the genes in cluster A and B (Supplemental Table 5 and Fig. 5a and b, left panels) correlate positively with NPI value, whereas those in cluster C correlate negatively (Supplemental Table 5 and Fig. 5c, left panel). Gene expression levels of the genes in the three clusters were also correlated with estrogen receptor (ER) status. High expression of the genes in cluster A and B correlated significantly with ER negativity whereas high expression level of the genes of cluster C correlated significantly with ER positivity (Figure 5a-c, right panels). The correlation between the expression and ER status was statistically significant also for individual genes in each of the three clusters ($P<0.001$).

4. Discussion

Fibroblast growth factor (FGF)-8 is expressed at an increased level in a high proportion of breast cancers (Marsh et al., 1999). In *in vitro* and *in vivo* breast cancer models, FGF-8 promotes proliferation, invasion and angiogenesis (Daphna-Iken et al., 1998; Mattila et al., 2001; Ruohola et al., 2001). However, little is known about the mechanistic role of FGF-8 in these processes. Here, we have undertaken gene expression profiling of S115 breast cancer cells treated with FGF-8b, from 1 to 24 hours, as a model for FGF-8-regulated breast cancer cells.

Our cDNA microarray analysis revealed a large number of significantly up- and down regulated genes in response to FGF-8b at all treatment times. In agreement with the role of FGF-8b as a mitogen, several of the most up regulated genes (e.g. epithelial membrane protein 1 (Emp1), Dusp4 and cyclin D) are proteins associated with proliferation and

tumorigenesis (Bartkova et al., 1994; Hippo et al., 2001; Wang et al., 2003; Wang et al., 1994). Correspondingly, antiproliferative genes such as Btg2 and genes with tumor suppressor functions such as Fibroblast growth factor 2 (FGFR2) (Eswarakumar et al., 2005) and Thrombospondin-1 (TSP-1) (Bleuel et al., 1999; Castle et al., 1997) were down regulated in response to FGF-8b (Supplemental table 2). We have earlier shown that silencing of FGFR2 expression in breast cancer cells markedly increases tumor growth in a nude mice tumor model (Tarkkonen, Nilsson et al., submitted manuscript) and FGFR2 protein is suppressed by FGF-8b in S115 breast cancer cells (unpublished data by EM. Nilsson). TSP-1 is a large glycoprotein secreted by various cell types. In normal mammalian tissue TSP-1 is a natural occurring angiogenic inhibitor which helps to maintain the normal quiescent vasculature (Bouck et al., 1996; Good et al., 1990; Hanahan and Folkman, 1996). Because of its antiangiogenic properties, overexpression of TSP-1 slows tumor growth in various experimental mouse models including breast cancer (Bleuel et al., 1999; Castle et al., 1997; Weinstat-Saslow et al., 1994; Volpert et al., 1998). Suppression of TSP-1 mRNA and protein in response to FGF-8b in breast cancer cells has also been shown in a previous study by our group (Mattila et al., 2006) which strengthens the finding of this study. Down regulation of genes with tumor suppressor functions such as TSP-1 and FGFR2 further supports a proliferative and tumorigenic function of FGF-8b.

Using the statistically most significant differentially regulated genes in a significance analysis of microarrays (SAM), the FGF-8b-regulated genes were arranged to functional categories and signaling pathways. The most significant FGF-8b-regulated genes were involved in categories and pathways related to cell cycle regulation, mitosis, cancer and cell death. Based on the results of the above analyses we chose six FGF-8b-regulated genes (Btg2, cyclin D1, cyclin B1, Plk1, aurora kinase A and Dusp4) for further analysis. The microarray data showed moderate to strong induction of cyclin D1, cyclin B1, Plk1, aurora kinase A and Dusp4 gene expression in response to FGF-8b. In contrast, Btg2 was transcriptionally repressed by FGF-8b. The results were validated in the same cell line (S115 cells) as well as in MCF-7 cells using quantitative PCR. Replication of the results in MCF-7 human breast

cancer cells demonstrates that the responses induced by FGF-8b are not cell line specific. Cyclin D1, cyclin B1, Plk1 and aurora kinase A also exhibited increased protein expression levels in response to FGF-8b.

Among the selected FGF-8b target genes Dual specificity phosphatase 4 (Dusp4) was the gene most up regulated by FGF-8b. Dusp4 belongs to the dual specificity phosphates (Dusp) subfamily which members are negative regulators of the mitogen activated protein (MAP) kinases MAPK/ERK, SAPK/JNK and p38 (Jeffrey et al., 2007). The strong upregulation of Dusp4 by FGF-8b at mRNA level in S115 and MCF-7 cells is likely a result of counterregulation of FGF-8b-induced activation of MAP kinases, in particular ERK1/2. As we did not observe regulation by FGF-8b at protein level, Dusp4 was not studied further experimentally. Although DUSP4 is often over expressed in breast cancer (Wang et al., 2003), we found its gene expression to correlate with ER positivity and inversely to poor prognosis (NPI) in a human breast cancer cohort (TRANSBIG).

Another gene strongly up regulated by FGF-8b was cyclin D1. Cyclin D1 plays a key role in the regulation of G1 to S phase progression of the cell cycle. It has also important cyclin-dependent kinase (CDK) -independent actions in cells through interactions with several transcription factors (Musgrove et al., 2011). Cyclin D1 is one of the most commonly overexpressed oncogenes in primary breast cancer, with overexpression in approximately 50% of the cases (Bartkova et al., 1994). Here we show that FGF-8b, similar to many other growth factors, enhances cyclin D1 transcript and protein in breast cancer cells. Furthermore, previous results from our laboratory show that blocking cyclin D1 reduces FGF-8b-stimulated proliferation (Nilsson et al., 2010). These findings indicate that cyclin D1 is a central actor in FGF-8b-mediated breast cancer cell growth and this prompted us to study whether silencing cyclin D1 influences the expression of the other selected FGF-8b-targets.

Silencing cyclin D1 decreased FGF-8b stimulation of expression of cyclin B1, Plk1 and aurora kinase A but interestingly, it did not affect expression of B-cell translocation gene 2 (Btg2). Btg2 belongs to the BTG/Tob family which in mammals comprises six proteins that regulate cell cycle progression (Winkler, 2010). BTG2 controls G1 to S phase progression

17

negatively by direct inhibition of cyclin D1 transcription (Guardavaccaro et al., 2000). Considering this, it is likely that induction of cyclin D1 by FGF-8b is a result of FGF-8b–mediated Btg2 repression. As one could expect, silencing of Btg2 in S115 cells increased the total cell number, although not significantly. Interestingly however, the mitogenic effect of FGF-8b was almost abolished in Btg2-silenced cells. This suggests that proper Btg2 expression is required for FGF-8b-mediated stimulation of proliferation. A loss of nuclear BTG2 expression is observed in ERα positive human breast tumors (Kawakubo et al., 2006), and an inverse correlation between breast tumor size and BTG2 expression has also been demonstrated (Kawakubo et al., 2006). BTG2 mRNA levels have been shown to be decreased by E2 and progestins in MCF-7 and T-47D breast cancer cells, respectively (Kawakubo et al., 2004). To the best of our knowledge this is however the first report on FGF-mediated repression of Btg2.

The late induction (12-24 hours after FGF-8b stimulation) of cyclin B1, Plk1 and aurora kinase A transcripts in S115 and MCF-7 cells is in accordance with the role of these genes as regulators of mitosis, which is a late event of the cell cycle. Cyclin B1, in complexes with cyclin dependent kinase 1 (cdk1), regulates early events of mitosis such as chromosome condensation, nuclear envelope breakdown and spindle pole assembly. Nuclear translocation of cyclin B1 has long been thought to be dependent on its phosphorylation by Plk1 (Toyoshima-Morimoto et al., 2001). Recent data suggest however that the nuclear import of cyclin B1 does not require Plk1 (Gavet and Pines, 2010). Plk1 belongs to the Polo like kinase family which in human has five identified members with roles in cell division. Plk1 and aurora kinases (aurora kinase A, aurora kinase B and aurora kinase C) co-regulate multiple processes in the dividing cell, such as entry into mitosis, mitotic spindle formation, sister chromatid resolution, chromosome-spindle connections and cytokinesis (reviewed in (Lens et al., 2010)). Here, we identified particularly Plk1 and aurora kinase A as FGF-8b targets. Both kinases are overexpressed in a large number of human tumors including breast cancer, and for most tumor types overexpression is associated with poor prognosis (Otto et al., 2009; Schvartzman et al., 2010; Strebhardt and Ullrich, 2006; Zhang et al., 2004; Zhang et al.,

2008). Silencing cyclin D1 in S115 cells abolished the inducing effect of FGF-8b (at 12 h) on Plk1 and reduced it on cyclin B1 and aurora kinase A protein suggesting that their induction by FGF-8b is dependent on or affected by cyclin D1. At a later time point (24 h) cyclin D1-silencing did not influence the effect of FGF-8b on cyclin B1 and aurora kinase A protein levels. This may be explained by usage of alternative pathways to obtain induction of cyclin B1 and aurora kinase A in the absence of cyclin D1. The role of cyclin D1 may be overtaken by cyclin D2 and/or cyclin D3 as D-type cyclins appear to have distinct, but overlapping functions (Lahti et al., 1997).

Silencing aurora kinase A in S115 cells significantly reduced elevation of the total cell number upon FGF-8b stimulation of the cells but did not block the FGF-8b-induced proliferation completely. This suggests that aurora kinase A plays an important role in FGF-8b-mediated cell proliferation but in its absence, proteins with redundant functions can overtake its actions. Plk1 might be one such protein as Aurora kinase A and Plk1 are shown to have redundant functions in activation of Cdk1 to promote entry into mitosis (Van Horn et al., 2010).

The evidence of aurora kinase A as a clinically important oncogene prompted us to explore the association between aurora kinase A and FGF-8b further. In S115 and MCF-7 tumors over expressing FGF-8b we found enhanced aurora kinase A immunoreactivity compared to tumors formed by mock-transfected cells. These results are in agreement with the enhanced mRNA and protein levels seen in FGF-8b-treated breast cancer cells and altogether our results suggest a strong association between aurora kinase A and FGF-8b. As reported earlier (Kimura et al., 1997; Sen et al., 1997), we found high levels of PLK1, aurora kinase A as well as aurora kinase B expression in human breast cancer specimens to correlate with poor prognosis. Furthermore, in a correlation with ER status we found their expression to correlate with ER negativity and this finding coincides with the fact that patients with ER negative breast tumors in general have a less favorable outcome than patients with ER positive breast tumors. The identification of these kinases as FGF-8b target genes is of great importance as they appear to be promising targets for anticancer therapy. Currently a large

19

number of inhibitors of PLK1, aurora kinase A and aurora kinase B are being evaluated in Phase I and Phase II trials (reviewed in Lens et al., 2010).

Analyses of mitotic progression and fidelity of cell division in the FGF-8b treated cell population indicated an elevated mitotic index in comparison to the non-stimulated cell population. This was likely due to the entry of cells into the cell cycle from the starvation culture conditions. Importantly, no obvious cell division errors were observed during short term cultures of the FGF-8b treated cells as the length of mitosis was comparable to the controls and the frequency of micronuclei was very low upon FGF-8b stimulation. Indirectly this proposes that the altered expression of FGF-8b target genes does not cause cell division defects during short term cultures. We however cannot exclude the possibility that the frequency of cell cycle/mitotic anomalies may increase in time when the cells have undergone more rounds of cell cycle after the FGF-8b stimulation. It is also important to note that aneuploidy caused by mitotic error can act both oncogenically and as a tumor suppressor depending on the level of induced cell division mistakes as well as the genetic background of the cells. Typically low rates of aneuploidy are associated with tumorigenesis while high rates of aneuploidy cause cell death and tumor suppression (Weaver and Cleveland, 2008; Weaver et al., 2007).

In a previous study (Nilsson et al., 2010) we showed that FGF-8b promotes cell cycle progression by signaling through the FGFR-Ras/MAPK and PI3K pathways and inducing transcription of D-type cyclins. Here, we extended our study on the mechanistic action of FGF-8b in tumorigenesis by performing a gene expression profiling of FGF-8b-treated breast cancer. The gene expression profiling revealed several differentially expressed genes in response to FGF-8b, which correlate with prognosis in human breast cancer. The most significantly up- and down regulated genes were related to cell cycle regulation, mitosis, cancer growth and cell death. We have provided evidence for FGF-8b-mediated down regulation of antiproliferative Btg2 which facilitates transcription of D-type cyclins. We also confirmed our previous findings on FGF-8b-mediated down regulation of TSP-1 and FGFR2 which potentially contributes to tumorigenesis. Furthermore, besides early cell cycle

20

regulators, we found FGF-8b to induce expression of late cell cycle phase genes that are critical for G2/M phase progression and completion of mitosis (e.g. cyclin B1, Plks and aurora kinases). We suggest an indirect regulation, mainly via cyclin D1, of these genes by FGF-8b.

In summary, this study demonstrates that besides stimulation of proliferation, FGF-8b contributes to tumorigenesis by repressing the expression of antiproliferative genes and indirectly by up regulating genes important for proper chromosomal segregation and cytokinesis. The FGF-8b-regulated genes identified in the study may thus provide therapeutic targets for FGF-8b-over expressing breast cancers.

References

Balslev, I., Axelsson, C.K., Zedeler, K., Rasmussen, B.B., Carstensen, B., Mouridsen, H.T., 1994. The Nottingham Prognostic Index applied to 9,149 patients from the studies of the Danish Breast Cancer Cooperative Group (DBCG). Breast Cancer Res. Treat. 32, 281-290.

Bartkova, J., Lukas, J., Muller, H., Lutzhoft, D., Strauss, M., Bartek, J., 1994. Cyclin D1 protein expression and function in human breast cancer. Int. J. Cancer 57, 353-361.

Bleuel, K., Popp, S., Fusenig, N.E., Stanbridge, E.J., Boukamp, P., 1999. Tumor suppression in human skin carcinoma cells by chromosome 15 transfer or thrombospondin-1 overexpression through halted tumor vascularization. Proc. Natl. Acad. Sci. U S A 96, 2065-2070.

Bouck, N., Stellmach, V., Hsu, S.C., 1996. How tumors become angiogenic. Adv Cancer Res 69, 135-174.

Castle, V.P., Dixit, V.M., Polverini, P.J., 1997. Thrombospondin-1 suppresses tumorigenesis and angiogenesis in serum- and anchorage-independent NIH 3T3 cells. Lab Invest 77, 51-61.

Daphna-Iken, D., Shankar, D.B., Lawshe, A., Ornitz, D.M., Shackleford, G.M., MacArthur, C.A., 1998. MMTV-Fgf8 transgenic mice develop mammary and salivary gland neoplasia and ovarian stromal hyperplasia. Oncogene 17, 2711-2717.

Desmedt, C., Piette, F., Loi, S., Wang, Y., Lallemand, F., Haibe-Kains, B., Viale, G., Delorenzi, M., Zhang, Y., d'Assignies, M.S., Bergh, J., Lidereau, R., Ellis, P., Harris, A.L., Klijn, J.G., Foekens, J.A., Cardoso, F., Piccart, M.J., Buyse, M., Sotiriou, C., 2007. Strong time dependence of the 76-gene prognostic signature for node-negative breast cancer patients in the TRANSBIG multicenter independent validation series. Clin. Cancer Res. 13, 3207-3214.

Dorkin, T.J., Robinson, M.C., Marsh, C., Bjartell, A., Neal, D.E., Leung, H.Y., 1999. FGF8 over-expression in prostate cancer is associated with decreased patient survival and persists in androgen independent disease. Oncogene 18, 2755-2761.

Elston, C.W., Ellis, I.O., 1991. Pathological prognostic factors in breast cancer. I. The value of histological grade in breast cancer: experience from a large study with long-term follow-up. Histopathology 19, 403-410.

Eswarakumar, V.P., Lax, I., Schlessinger, J., 2005. Cellular signaling by fibroblast growth factor receptors. Cytokine Growth Factor Rev. 16, 139-149.

Galea, M.H., Blamey, R.W., Elston, C.E., Ellis, I.O., 1992. The Nottingham Prognostic Index in primary breast cancer. Breast Cancer Res. Treat. 22, 207-219.

Gavet, O., Pines, J., 2010. Activation of cyclin B1-Cdk1 synchronizes events in the nucleus and the cytoplasm at mitosis. J Cell Biol 189, 247-259.

Gemel, J., Gorry, M., Ehrlich, G.D., MacArthur, C.A., 1996. Structure and sequence of human FGF8. Genomics 35, 253-257.

Gentleman, R.C., Carey, V.J., Bates, D.M., Bolstad, B., Dettling, M., Dudoit, S., Ellis, B., Gautier, L., Ge, Y., Gentry, J., Hornik, K., Hothorn, T., Huber, W., Iacus, S., Irizarry, R., Leisch, F., Li, C., Maechler, M., Rossini, A.J., Sawitzki, G., Smith, C., Smyth, G., Tierney, L., Yang, J.Y., Zhang, J., 2004. Bioconductor: open software development for computational biology and bioinformatics. Genome Biol. 5, R80.

Giri, D., Ropiquet, F., Ittmann, M., 1999. Alterations in expression of basic fibroblast growth factor (FGF) 2 and its receptor FGFR-1 in human prostate cancer. Clin. Cancer Res. 5, 1063-1071.

Good, D.J., Polverini, P.J., Rastinejad, F., Le Beau, M.M., Lemons, R.S., Frazier, W.A., Bouck, N.P., 1990. A tumor suppressor-dependent inhibitor of angiogenesis is immunologically and functionally indistinguishable from a fragment of thrombospondin. Proc. Natl. Acad. Sci. U S A 87, 6624-6628.

Guardavaccaro, D., Corrente, G., Covone, F., Micheli, L., D'Agnano, I., Starace, G., Caruso, M., Tirone, F., 2000. Arrest of G(1)-S progression by the p53-inducible gene PC3 is Rb dependent and relies on the inhibition of cyclin D1 transcription. Mol Cell Biol 20, 1797-1815.

Hanahan, D., Folkman, J., 1996. Patterns and emerging mechanisms of the angiogenic switch during tumorigenesis. Cell 86, 353-364.

Hippo, Y., Yashiro, M., Ishii, M., Taniguchi, H., Tsutsumi, S., Hirakawa, K., Kodama, T., Aburatani, H., 2001. Differential gene expression profiles of scirrhous gastric cancer cells with high metastatic potential to peritoneum or lymph nodes. Cancer Res. 61, 889-895.

Jeffrey, K.L., Camps, M., Rommel, C., Mackay, C.R., 2007. Targeting dual-specificity phosphatases: manipulating MAP kinase signalling and immune responses. Nat. Rev. Drug. Discov. 6, 391-403.

Katoh, Y., Katoh, M., 2009. FGFR2-related pathogenesis and FGFR2-targeted therapeutics (Review). Int. J. Mol. Med. 23, 307-311.

Kawakubo, H., Brachtel, E., Hayashida, T., Yeo, G., Kish, J., Muzikansky, A., Walden, P.D., Maheswaran, S., 2006. Loss of B-cell translocation gene-2 in estrogen receptor-positive breast carcinoma is associated with tumor grade and overexpression of cyclin d1 protein. Cancer Res. 66, 7075-7082.

Kawakubo, H., Carey, J.L., Brachtel, E., Gupta, V., Green, J.E., Walden, P.D., Maheswaran, S., 2004. Expression of the NF-kappaB-responsive gene BTG2 is aberrantly regulated in breast cancer. Oncogene 23, 8310-8319.

Kimura, M., Matsuda, Y., Eki, T., Yoshioka, T., Okumura, K., Hanaoka, F., Okano, Y., 1997. Assignment of STK6 to human chromosome 20q13.2-->q13.3 and a pseudogene STK6P to 1q41-->q42. Cytogenet. Cell Genet. 79, 201-203.

Lahti, J.M., Li, H., Kidd, V.J., 1997. Elimination of cyclin D1 in vertebrate cells leads to an altered cell cycle phenotype, which is rescued by overexpression of murine cyclins D1, D2, or D3 but not by a mutant cyclin D1. J Biol Chem 272, 10859-10869.

Lens, S.M., Voest, E.E., Medema, R.H., 2010. Shared and separate functions of polo-like kinases and aurora kinases in cancer. Nat. Rev. Cancer 10, 825-841.

Marsh, S.K., Bansal, G.S., Zammit, C., Barnard, R., Coope, R., Roberts-Clarke, D., Gomm, J.J., Coombes, R.C., Johnston, C.L., 1999. Increased expression of fibroblast growth factor 8 in human breast cancer. Oncogene 18, 1053-1060.

Marzioni, D., Lorenzi, T., Mazzucchelli, R., Capparuccia, L., Morroni, M., Fiorini, R., Bracalenti, C., Catalano, A., David, G., Castellucci, M., Muzzonigro, G., Montironi, R., 2009. Expression of basic fibroblast growth factor, its receptors and syndecans in bladder cancer. Int. J. Immunopathol. Pharmacol. 22, 627-638.

Mattila, M.M., Harkonen, P.L., 2007. Role of fibroblast growth factor 8 in growth and progression of hormonal cancer. Cytokine Growth Factor Rev 18, 257-266.

Mattila, M.M., Ruohola, J.K., Valve, E.M., Tasanen, M.J., Seppanen, J.A., Harkonen, P.L., 2001. FGF-8b increases angiogenic capacity and tumor growth of androgen-regulated S115 breast cancer cells. Oncogene 20, 2791-2804.

Mattila, M.M., Tarkkonen, K.M., Seppanen, J.A., Ruohola, J.K., Valve, E.M., Harkonen, P.L., 2006. Androgen and fibroblast growth factor 8 (FGF8) downregulation of thrombospondin 1 (TSP1) in mouse breast cancer cells. Mol Cell Endocrinol 253, 36-43.

Musgrove, E.A., Caldon, C.E., Barraclough, J., Stone, A., Sutherland, R.L., 2011. Cyclin D as a therapeutic target in cancer. Nat. Rev. Cancer 11, 558-572.

Nilsson, E.M., Brokken, L.J., Harkonen, P.L., 2010. Fibroblast growth factor 8 increases breast cancer cell growth by promoting cell cycle progression and by protecting against cell death. Exp. Cell Res. 316, 800-812.

Olsen, S.K., Li, J.Y., Bromleigh, C., Eliseenkova, A.V., Ibrahimi, O.A., Lao, Z., Zhang, F., Linhardt, R.J., Joyner, A.L., Mohammadi, M., 2006. Structural basis by which alternative splicing modulates the organizer activity of FGF8 in the brain. Genes Dev. 20, 185-198.

Otto, T., Horn, S., Brockmann, M., Eilers, U., Schuttrumpf, L., Popov, N., Kenney, A.M., Schulte, J.H., Beijersbergen, R., Christiansen, H., Berwanger, B., Eilers, M., 2009. Stabilization of N-Myc is a critical function of Aurora A in human neuroblastoma. Cancer Cell 15, 67-78.

Ruohola, J.K., Viitanen, T.P., Valve, E.M., Seppanen, J.A., Loponen, N.T., Keskitalo, J.J., Lakkakorpi, P.T., Harkonen, P.L., 2001. Enhanced invasion and tumor growth of fibroblast growth factor 8b-overexpressing MCF-7 human breast cancer cells. Cancer Res. 61, 4229-4237.

Saal, L.H., Troein, C., Vallon-Christersson, J., Gruvberger, S., Borg, A., Peterson, C., 2002. BioArray Software Environment (BASE): a platform for comprehensive management and analysis of microarray data. Genome Biol. 3, SOFTWARE0003.

Saeed, A.I., Sharov, V., White, J., Li, J., Liang, W., Bhagabati, N., Braisted, J., Klapa, M., Currier, T., Thiagarajan, M., Sturn, A., Snuffin, M., Rezantsev, A., Popov, D., Ryltsov, A., Kostukovich, E., Borisovsky, I., Liu, Z., Vinsavich, A., Trush, V., Quackenbush, J., 2003. TM4: a free, open-source system for microarray data management and analysis. Biotechniques 34, 374-378.

Sauerbrei, W., Hubner, K., Schmoor, C., Schumacher, M., 1997. Validation of existing and development of new prognostic classification schemes in node negative breast cancer. German Breast Cancer Study Group. Breast Cancer Res. Treat. 42, 149-163.

Schvartzman, J.M., Sotillo, R., Benezra, R., 2010. Mitotic chromosomal instability and cancer: mouse modelling of the human disease. Nat. Rev. Cancer 10, 102-115.

Sen, S., Zhou, H., White, R.A., 1997. A putative serine/threonine kinase encoding gene BTAK on chromosome 20q13 is amplified and overexpressed in human breast cancer cell lines. Oncogene 14, 2195-2200.

Strebhardt, K., Ullrich, A., 2006. Targeting polo-like kinase 1 for cancer therapy. Nat. Rev. Cancer 6, 321-330.

Team, R.D.C. (2009). R: a language and environment for statistical computing (R Development Core Team, R Foundation for Statistical Computing).

Todd, J.H., Dowle, C., Williams, M.R., Elston, C.W., Ellis, I.O., Hinton, C.P., Blamey, R.W., Haybittle, J.L., 1987. Confirmation of a prognostic index in primary breast cancer. Br. J. Cancer 56, 489-492.

Toyoshima-Morimoto, F., Taniguchi, E., Shinya, N., Iwamatsu, A., Nishida, E., 2001. Polo-like kinase 1 phosphorylates cyclin B1 and targets it to the nucleus during prophase. Nature 410, 215-220.

Van Horn, R.D., Chu, S., Fan, L., Yin, T., Du, J., Beckmann, R., Mader, M., Zhu, G., Toth, J., Blanchard, K., Ye, X.S., 2010. Cdk1 activity is required for mitotic activation of aurora A during G2/M transition of human cells. J. Biol. Chem. 285, 21849-21857.

Wang, H.Y., Cheng, Z., Malbon, C.C., 2003. Overexpression of mitogen-activated protein kinase phosphatases MKP1, MKP2 in human breast cancer. Cancer Lett 191, 229-237.

Wang, T.C., Cardiff, R.D., Zukerberg, L., Lees, E., Arnold, A., Schmidt, E.V., 1994. Mammary hyperplasia and carcinoma in MMTV-cyclin D1 transgenic mice. Nature 369, 669-671.

Weaver, B.A., Cleveland, D.W., 2008. The aneuploidy paradox in cell growth and tumorigenesis. Cancer Cell 14, 431-433.

Weaver, B.A., Silk, A.D., Montagna, C., Verdier-Pinard, P., Cleveland, D.W., 2007. Aneuploidy acts both oncogenically and as a tumor suppressor. Cancer Cell 11, 25-36.

Weinstat-Saslow, D.L., Zabrenetzky, V.S., VanHoutte, K., Frazier, W.A., Roberts, D.D., Steeg, P.S., 1994. Transfection of thrombospondin 1 complementary DNA into a human breast carcinoma cell line reduces primary tumor growth, metastatic potential, and angiogenesis. Cancer Res. 54, 6504-6511.

Winkler, G.S., 2010. The mammalian anti-proliferative BTG/Tob protein family. J. Cell Physiol. 222, 66-72.

Volpert, O.V., Lawler, J., Bouck, N.P., 1998. A human fibrosarcoma inhibits systemic angiogenesis and the growth of experimental metastases via thrombospondin-1. Proc. Natl. Acad. Sci. U S A 95, 6343-6348.

Zhang, D., Hirota, T., Marumoto, T., Shimizu, M., Kunitoku, N., Sasayama, T., Arima, Y., Feng, L., Suzuki, M., Takeya, M., Saya, H., 2004. Cre-loxP-controlled periodic Aurora-A overexpression induces mitotic abnormalities and hyperplasia in mammary glands of mouse models. Oncogene 23, 8720-8730.

Zhang, D., Shimizu, T., Araki, N., Hirota, T., Yoshie, M., Ogawa, K., Nakagata, N., Takeya, M., Saya, H., 2008. Aurora A overexpression induces cellular senescence in mammary gland hyperplastic tumors developed in p53-deficient mice. Oncogene 27, 4305-4314.

Figure legends

FIGURE 1. Relative mRNA expression of Btg2, cyclin D1, cyclin B1, Plk1, aurora kinase A and Dusp4 in S115 cells as measured by (a) cDNA microarrays and (b) qPCR. c) Relative mRNA expression in MCF-7 cells measured by qPCR. Total RNA was extracted from S115 cells treated with FGF-8b for 1, 3, 6, 12, and 24 hours. RNA was converted to cDNA which then were used for cDNA microarray analysis and quantitative PCR analysis, respectively. Data are shown as fold change by FGF-8b as compared to control. * in Figure a indicates FDR<0.05.

FIGURE 2. FGF-8b regulation of BTG2, cyclin D1, cyclin B1, Plk1 and aurora kinase A protein. (a) S115 cells were treated with siRNA targeting cyclin D1 followed by FGF-8b treatment for 12 and 24 hours. Total protein was isolated, subjected to SDS-PAGE and probed with antibodies against BTG2, cyclin D1, cyclin B1, Plk1, aurora kinase A and β-actin. (b) S115 and MCF-7 cells either mock-transfected or over expressing FGF-8b were grown subcutaneously as nude mouse tumors. Sections of formalin-fixed paraffin embedded S115-mock, S115-FGF-8b, MCF-7-mock and MCF-7-FGF-8b tumors were immunostained for aurora kinase A. Scale bar, 50 μm.

FIGURE 3. Progression and fidelity of mitosis in control and FGF-8b treated mouse S115 cells. (a) Mitotic index is significantly (P=0.008) elevated upon FGF-8b stimulation. The diagram shows the average mitotic index in percentages in control and FGF-8b treated cell populations. The micrographs on the right hand side show representative images of DAPI stained cell populations. The arrows denote mitotic cells. Scale bar, 50 μm. (b) The diagram shows the average duration of mitosis in minutes in control and FGF-8b treated cell populations. The micrographs on the right hand side show representative still images from the live cell time-lapse films. The white circles surround a cell in both growth conditions that undergoes normal cell division. Scale bar, 100 μm. (c) The average frequency of micronuclei in control and FGF-8b treated cell populations. The micrographs on the right hand side show representative images of control and FGF-8b treated cell populations. The arrows denote micronuclei. Scale bar, 20 μm.

FIGURE 4. The effect of Btg2, aurora kinase A and cyclin D1 gene silencing on FGF-8b-regulated cell proliferation and cell survival. The Btg2, aurora kinase A and cyclin D1 genes were silenced with siRNA in S115 cells. The left panels of Figure a, b and c show the protein expression of BTG2, aurora kinase A and cyclin D1, respectively, 48 h after siRNA transfection. a and b, right panel) Btg2 and aurora kinase A-silenced cells were stimulated with FGF-8b to induce cell proliferation 24 h after siRNA transfection. After additional 48 h the number of viable cells was counted using the trypan blue exclusion method. c, right panel) 24 h after siRNA transfection cyclin D1-silenced cells were simultaneously treated with staurosporine (STS) and FGF-8b. Cell survival promoted by FGF-8b was measured using the trypan blue exclusion method. The statistical differences were tested using one-way ANOVA followed by Bonferroni's multiple comparison test. Bars marked with the same letter do not differ significantly (P<0.05).

FIGURE 5. Distribution of expression levels of genes in the three different gene sets A-C (derived from hierarchical clustering in Supplemental Figure 2) and NPI values (left panels) and ER status (right panels) of tumors visualized as box plots (a-c). 0, ER-negative tumors; 1, ER-positive tumors.

TABLE 1. The 20 most differentially-expressed genes in response to treatment with FGF-8b for 1-24 hours.
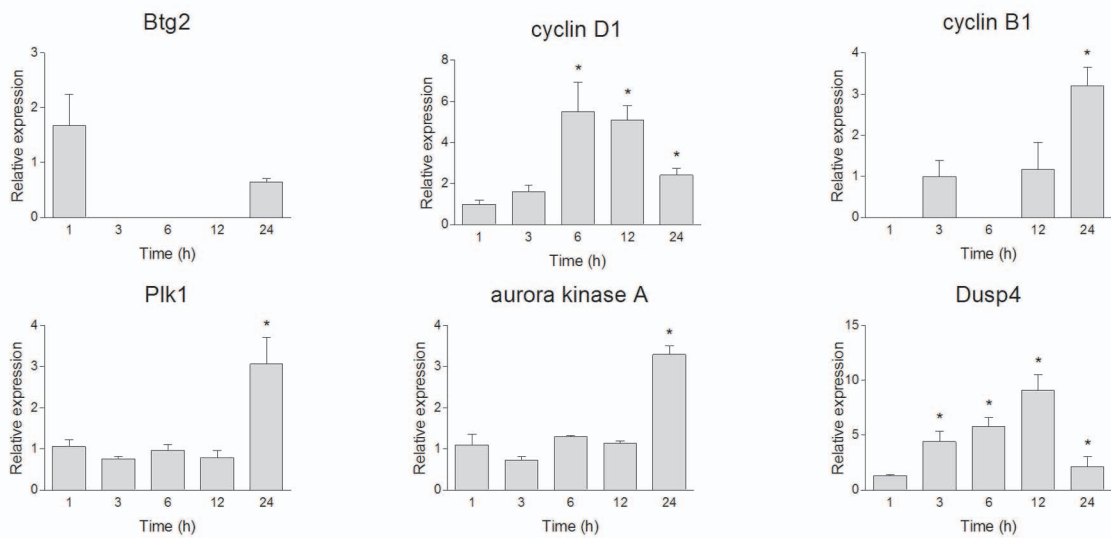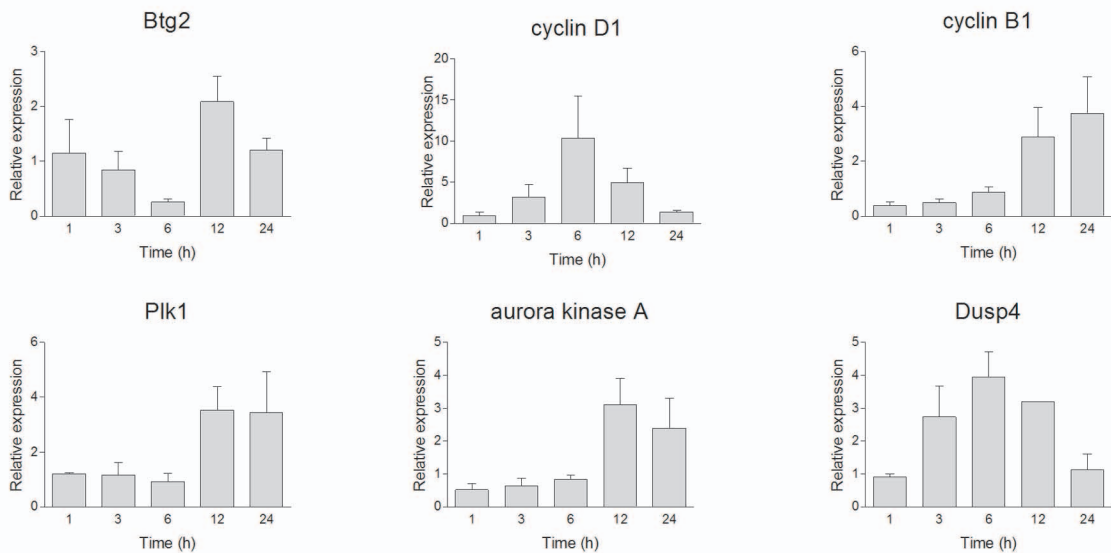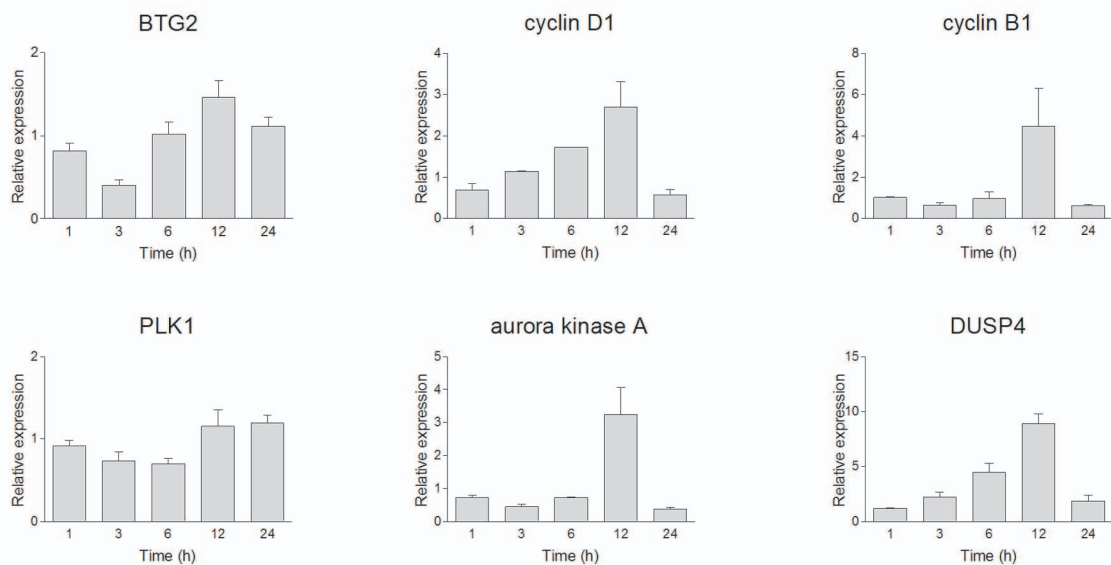
Gene symbol	Name	Accession no	P-value
Aurka	aurora kinase A	NM_011497	0
Tacc3	transforming acidic coiled-coil containing protein 3	NM_011524	0
Ccnb2	cyclin B2	NM_007630	1.11E-16
Pttg1	pituitary tumor-transforming 1	NM_013917	1.11E-16
Tnfaip2	tumor necrosis factor α 2	NM_009396	3.33E-16
Tubb6	tubulin β 6	NM_026473	3.33E-16
Hmga1	high mobility group AT-hook 1	NM_016660	6.66E-16
Trim16	tripartite motif-containing 16		1.33E-15
Birc5	baculoviral IAP repeat-containing 5	NM_009689	1.89E-15
Csf1	colony stimulating factor 1	NM_007778	2.78E-15
Mcm5	minichromosome maintenance complex component 5	NM_008566	1.75E-14
Cdc45l	cell division cycle 45-like	NM_009862	1.83E-14
Fgfr1	fibroblast growth factor receptor 1		4.61E-14
Cdca8	cell division cycle associated 8	NM_026560	4.80E-14
Cenpa	centromere protein A	NM_007681	7.02E-14
Nek2	NIMA (never in mitosis gene a)-related kinase 2	NM_010892	7.48E-14
Cyr61	cysteine-rich angiogenic inducer 61	NM_010516	8.40E-14
Kif22	kinesin family member 22	NM_145588	8.79E-14
Apcdd1	adenomatosis polyposis coli down-regulated 1		9.85E-14
Ctgf	connective tissue growth factor	NM_010217	9.96E-14
Pvr	poliovirus receptor	NM_009310	1.07E-13
Gdpd2	glycerophosphodiester phosphodiesterase domain containing 2	NM_023608	1.13E-13
Stc2	stanniocalcin 2	NM_011491	1.22E-13
Acpl2	acid phosphatase-like 2	NM_153420	2.12E-13
Glrx	glutaredoxin	NM_053108	3.10E-13
Bcl2l11	BCL2 (B-cell CLL/lymphoma 2)-like 11	NM_009754	4.95E-13
Myc	v-myc myelocytomatosis viral oncogene homolog	NM_010849	5.50E-13
Lmcd1	IM and cysteine-rich domains 1	NM_144799	5.82E-13
Pola2	polymerase alpha 2	NM_008893	6.62E-13
Cdca5	cell division cycle associated 5	NM_026410	8.50E-13
Rad54l	RAD54-like	NM_009015	1.15E-12
Cdc20	cell division cycle 20 homolog	NM_023223	1.24E-12
Arhgap22	Rho GTPase activating protein 22	NM_153800	1.26E-12
Mybl2	v-myb myeloblastosis viral oncogene homolog-like 2	NM_008652	1.32E-12
Tk1	thymidine kinase 1	NM_009387	1.38E-12
Aurkb	aurora kinase B	NM_011496	1.46E-12
Efnb1	ephrin-B1	NM_010110	1.51E-12
Prelp	proline/arginine-rich end leucine-rich repeat protein	NM_054077	1.57E-12
Cenpm	centromere protein M	NM_025639,NM_178269	1.64E-12
Rasa3	RAS p21 protein activator 3	NM_009025	2.22E-12

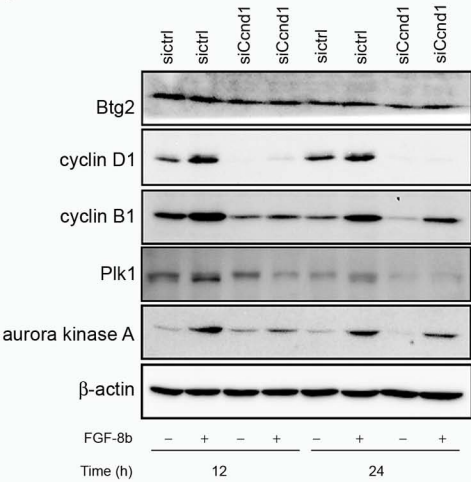**TABLE 2.** Five functional categories associated with the most significantly altered FGF-8b-regulated genes.

Category	P-value	Genes
Cell cycle	1.79E-14 - 1.95E-02	NGF, BUB1B, CKS2, GADD45G, CDCA5, BCL2L1, ERCC1, UHRF1, TACC3, PLK1, CDT1, PTTG1, TUBG1, CDKN2D, CDC25B, MYC, PVR, AURKA, FOXM1, ESPL1, FANCA, PSRC1, CSF1, AURKB, CCNA2, PTEN, ATF3, SIK1, SPARC, SMAD3, BCL2L11, CCND1, CYP26B1, PLK2, CRYAB, TGIF1, SUV39H1, H2AFX, KIFC1, JUN, DCLK1, CKS1B, ID1, ERRFI1, BIRC5, PPAP2A, MYBL2, E2F4
Cancer	5.03E-14 - 2.16E-02	IER3, TYMS, CKS2, SAA1, BCL2L1, BIN1, TNS1, BTG2, NF2, TNFRSF9, PTCH1, MGAT3, GLRX, CDKN2D, MYC, PTPN1, NDRG1, LGALS3, CLU, AURKB, CCNA2, DDIT4, ATF3, FOSL1, CCNB2, BCL2L11, CRYAB, ETS2, DUSP1, H2AFX, INCENP, CKS1B, BIRC5, ID1, NGF, BUB1B, PLK1, CST3, CDC20, TK1, LIG1, PTTG1, CDC6, CDCA7, CDC25B, FGFR2, AURKA, APCDD1, FOXM1, LIF, CSF1, PLAUR, PTEN, SRM, SLC2A1, SMAD3, CCND1, FGFR1, VDR, JUN, TIMP2, BHLHE40, HMGA1
Cellular growth and proliferation	6.41E-09 - 2.2E-02	CD81, CKS2, BCL2L1, BTG2, FOSL2, SHB, NF2, TACC3, TNFRSF9, PTCH1, KLF5, CDKN2D, MYC, NDRG1, PTPN1, LGALS3, ESPL1, FANCA, PSRC1, CLU, CCNA2, ATF3, FOSL1, ZFP36L1, CXCL10, TACC2, BCL2L11, MXD3, CRYAB, HBEGF, YPEL3, ETS2, DUSP1, SOX4, CKS1B, BIRC5, ID1, NGF, CDK2AP1, STMN1, ERCC1, ZMAT3, UHRF1, EFNB1, CST3, GRN, PTTG1, LPIN1, WNT7B, CDC25B, ARHGAP22, FGFR2, AURKA, PVR, SOX9, APCDD1, FOXM1, LIF, CSF1, PTEN, PLK3, ATF4, SPARC, SMAD3, DUSP10, TRAF5, CCND1, VDR, FGFR1, PLK2, LDLR, IL12RB1, TGIF1, GABPB2, NUP62, JUN, TIMP2, HMGA1, VASP, MYBL2, E2F4
Cell death	5.89E-06 - 2.16E-02	IER3, EME1, BCL2L1, TNFRSF9, ATP2B4, KAT2A, KLF5, CDKN2D, MYC, PTPN1, LGALS3, TNNT2, FANCA, CLU, DUSP4, DDIT4, ST3GAL1, ATF3, UNG, FOSL1, SOAT1, BCL2L11, CYR61, CRYAB, MXD3, DUSP1, BIRC5, NGF, PPIF, CDK2AP1, STMN1, ERCC1, UHRF1, PLK1, DUSP6, ATG7, CDC25B, FGFR2, SOX9, AURKA, LIF, CSF1, LBP, PTEN, PLK3, SLC2A1, SPARC, SMAD3, TRAF5, CCND1, FGFR1, CYP26B1, VDR, LDLR, ARRB1, JUN, BHLHE40, HMGA1, NRF1, FEN1
Tumor morphology	6.54E-06 - 1.95E-02	IER3, BUB1B, BCL2L1, TNS1, BTG2, NF2, CST3, PLK1, TNFRSF9, PTCH1, MGAT3, CDC25B, FGFR2, MYC, PTPN1, AURKA, NDRG1, FOXM1, LGALS3, CSF1, CLU, PLAUR, PTEN, SMAD3, CCND1, BCL2L11, FGFETS2, JUN, TIMP2, HMGA1, ID1, BIRC5

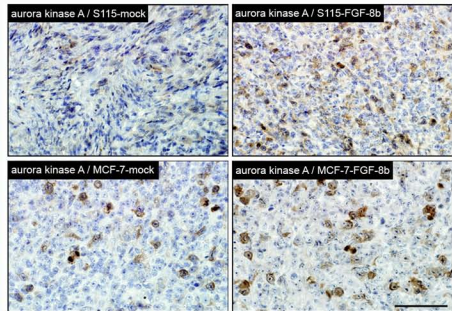**TABLE 3.** Canonical pathways associated with the most significantly altered FGF-8b-regulated genes.

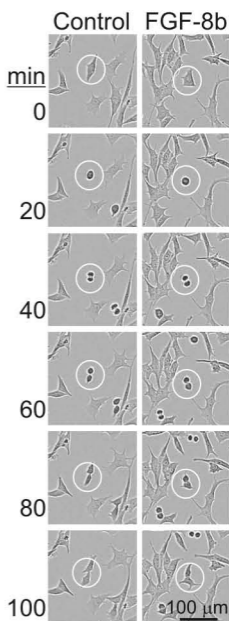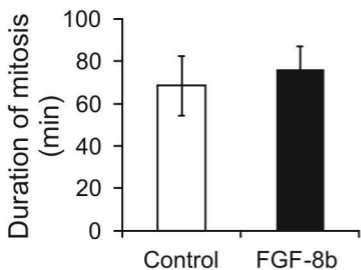| Ingenuity Canonical Pathways	P-value	Genes
Mitotic roles of Polo-like kinase	4.1E-04	PKMYT1, CDC25B, CCNB2, PLK1, CDC20, ESPL1, PLK2, PTTG1
Cell cycle regulation by BTG family proteins	1.2E-03	PRMT1, BTG2, CCND1, CCRN4L, E2F4
Role of BRCA1 in DNA damage response	1.4E-03	RFC3, RFC5, PLK1, FANCA, RFC2, E2F4
Small cell lung cancer signaling	1.4E-03	SUV39H1, MYC, BCL2L1, CCND1, TRAF5, CKS1B, PTEN
ATM signaling	1.5E-03	GADD45G, H2AFX, ATF4, JUN, MDC1CCNB2
Molecular mechanisms of cancer	3.3E-03	BCL2L1, SMAD3, BCL2L11, CCND1, ARHGEF7, PTCH1, ARHGEF19, SUV39H1, CDKN2D, CDC25B, MYC, PLCB4, AURKA, JUN, RAPGEF3, PAK4, E2F4
p53 signaling	4.3E-03	GADD45G, BCL2L1, JUN, CCND1, BIRC5, PTEN, FASN
Pyrimidine metabolism	4.9E-03	TYMS, PRIM2, RFC3, POLD2, POLA2, RFC5, TK1DTYMK, UNG
Methane metabolism	5.5E-03	PRDX5, SHMT1, SHMT2
Circadian rhythm signaling	6.7E-03	BHLHE41, ATF4, BHLHE40, CSNK1E
Role of CHK proteins in cell cycle checkpoint control	8.5E-03	RFC3, RFC5, RFC2, E2F4

a

	sictrl	sictrl	siCcnd1	siCcnd1	sictrl	sictrl	siCcnd1	siCcnd1

Btg2

cyclin D1

cyclin B1

Plk1

aurora kinase A

β-actin

FGF-8b   −   +   −   +   −   +   −   +

Time (h)   12   24

b

aurora kinase A / S115-mock

aurora kinase A / S115-FGF-8b

aurora kinase A / MCF-7-mock

aurora kinase A / MCF-7-FGF-8b

a

Mitotic index (%)

Control   FGF-8b

***

Control

FGF-8b

50 μm

b

Duration of mitosis (min)

Control   FGF-8b

Control FGF-8b

min

0

20

40

60

80

100

100 μm

c

Frequency of micronulei (%)

Control   FGF-8b

Control

FGF-8b

20 μm

a

BTG2

β-actin

sicontrol | siBtg2

Cell number (x1000)

- control
- FGF-8b

sicontrol   siBtg2

b

aurora kinase A

β-actin

sicontrol | siAurka

Cell number (x1000)

- control
- FGF-8b

sicontrol   siAurka

c

cyclin D1

β-actin

sicontrol | siCcnd1

Trypan blue positive cells (%)

- control
- FGF-8b
- STS
- STS+FGF-8b

sicontrol   siCcnd1
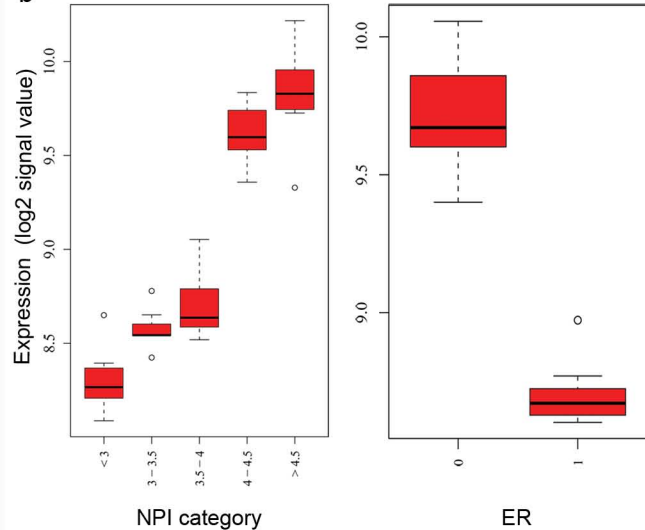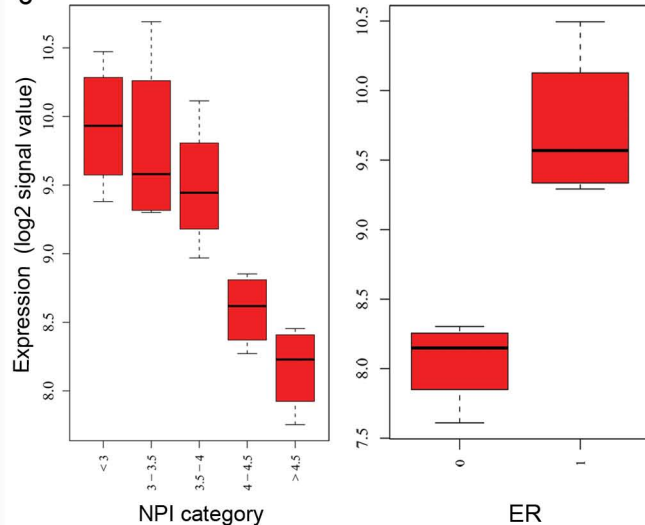
Genes in cluster A
V-myb myeloblastosis viral oncogene
homolog (avian)-like 2
Baculoviral IAP repeat-containing 5
Polo-like kinase 1 (Drosophila)
Cyclin A2
Fanconi anemia, complementation group A
Cell division cycle 6 homolog (S. cerevisiae)
Chromatin assembly factor 1, subunit B (p60)
Aurora kinase B
Kinesin family member C1
Chromatin licensing and DNA replication factor 1
NIMA (never in mitosis gene a)-related kinase 2
Cyclin A2
Centromere protein M
Cell division cycle associated 3
Cell division cycle associated 8

Genes in cluster B
Baculoviral IAP repeat-containing 5
Thymidine kinase 1, soluble
Cyclin B2
Cell division cycle 20 homolog (S. cerevisiae)
Aurora kinase A
Kinesin family member 2C

Genes in cluster C
Stanniocalcin 2
Dual Specificity Phosphatase 4